

Modeling of End-On (μ -Peroxo)dicopper(II) Complexes

Peter Comba,^{*,1a} Peter Hilfenhaus,^{1a} and Kenneth D. Karlin^{1b}

Anorganisch-Chemisches Institut der Universität, Im Neuenheimer Feld 270, D-69120 Heidelberg, Germany, and Department of Chemistry, The Johns Hopkins University, Baltimore, Maryland 21218

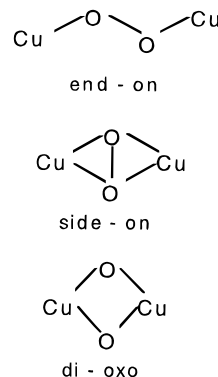
Received October 31, 1996[®]

A force field for (μ -peroxo)dicopper(II) complexes was developed, based on a well-established parameter set for copper(II) complexes, the structural and spectroscopic data of a (μ -peroxo)dicopper(II) complex with tris(2-pyridylmethylamine) donors and a series of (μ -peroxo)dicobalt(III) compounds. This force field is shown to well reproduce the structural properties of the available structures of (μ -peroxo)dicopper(II) and (μ -peroxo)dicobalt(III) complexes, and it was used to compute a series of (μ -peroxo)dicopper(II) compounds with two tris(2-pyridylmethylamin) units linked by different organic spacers at a 5-pyridyl position at each tetradentate moiety. The computed structures and strain energies indicate that (i) in the compound with an ethyl spacer group the ligand induces a considerable strain and distortion in the μ -peroxo product, and these effects compensate the favorable entropy effects due to the ligand preorganization, in agreement with the published experimental results; (ii) the (μ -peroxo)dicopper(II) compound with the propyl-linked ligand is relatively unstrained and structurally very similar to the parent compound; and (iii) larger spacer groups lead to rather distorted (μ -peroxo)dicopper(II) products.

Introduction

There is an increasing interest in the activation of dioxygen by dicopper(I) compounds, and structural, thermodynamic, and mechanistic aspects of a number of systems that are believed to be relevant for oxidative chemical processes and/or metalloenzyme active site modeling have been reported.² Three structural modes of dicopper(I)–dioxygen adducts have been discussed, end-on (μ -peroxo)dicopper(II),^{3a} side-on (μ -peroxo)dicopper(II),^{3b,c} and di-(μ -oxo)dicopper(III),^{3d} see Chart 1. Structural, spectroscopic, kinetic, and thermodynamic features of these structural types have been reported,^{3,4} and compared to experimentally determined data of oxygenated forms of arthropodal and molluscan hemocyanine active sites.⁵ A focal point in the study of dicopper(I)–dioxygen adducts is to

Chart 1



understand the correlation between the structural characteristics of the copper chromophores and the stability and reactivity of these species. In this report, we concentrate on molecular mechanics models of the (μ -peroxo)dicopper(II) (end-on) mode and the question of how this may be stabilized by the ligand coordinated to the copper centers. The specific question to be answered here is based on a recent study, aimed at stabilizing the (μ -peroxo)dicopper(II) species by linking the two tripodal chromophores by an organic spacer group (Scheme 1).^{4c} The kinetic and thermodynamic data of the ligand involving an ethyl spacer indicate that the favorable entropic effect was cancelled by a disfavorable enthalpic effect, possibly due to ligand-induced strain.^{4c} A careful design, based on these experimental results, and involving molecular mechanics calculations, might be able to provide insight in attempting to overcome these problems.

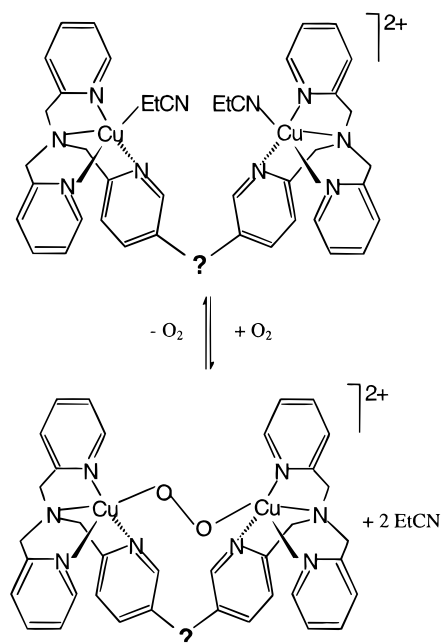
Molecular mechanics modeling of coordination compounds has made much progress in the last decade, and it has now reached a stage where reliable results may be obtained in many areas of applications.⁶ One of the features and possible problems of molecular mechanics is that these computations are based on an arbitrary but well-chosen and documented set

[®] Abstract published in *Advance ACS Abstracts*, April 1, 1997.

- (1) (a) University of Heidelberg. (b) The Johns Hopkins University.
 (2) (a) Kitajima, N.; Moro-oka, Y. *Chem. Rev.* **1994**, *94*, 737. (b) *Bioinorganic Chemistry of Copper*; Karlin, K. D., Tyeklár, Z., Eds.; Chapman & Hall: New York, 1993. (c) *Bioinorganic Catalysis*; Reedijk, J., Ed.; Marcel Dekker: New York, Hong Kong, 1993. (d) Vigato, P. A.; Tamburini, S.; Fenton, D. E. *Coord. Chem. Rev.* **1990**, *106*, 25. (e) Sorrell, T. N. *Tetrahedron* **1989**, *45*, 3.
 (3) (a) Tyeklár, Z.; Jacobson, R. R.; Wei, N.; Murthy, N. N.; Zubieta, J.; Karlin, K. D. *J. Am. Chem. Soc.* **1993**, *115*, 2677. (b) Kitajima, N.; Fujisawa, K.; Moro-oka, K.; Toriumi, K. *J. Am. Chem. Soc.* **1989**, *111*, 8975. (c) Kitajima, N.; Fujisawa, K.; Fujimoto, C.; Moro-oka, Y.; Hashimoto, S.; Kitagawa, T.; Toriumi, K.; Tatum, K.; Nakamura, A. *J. Am. Chem. Soc.* **1992**, *114*, 1277. (d) Halfen, J. A.; Mahapatra, S.; Wilkinson, E. C.; Kaderli, S.; Young, V. G., Jr.; Que, L., Jr.; Zuberbühler, A. D.; Tolman, W. B. *Science* **1996**, *271*, 1397.
 (4) (a) Menif, R.; Martell, A. E.; Squattrito, P. J.; Clearfield, A. *Inorg. Chem.* **1993**, *29*, 4723. (b) Comba, P.; Hambley, T. W.; Hilfenhaus, P.; Richens, D. T. *J. Chem. Soc., Dalton Trans.* **1996**, 533. (c) Lee, D.-H.; Wei, N.; Murthy, N. N.; Tyeklár, Z.; Karlin, K. D.; Kaderli, S.; Jung, B.; Zuberbühler, A. D. *J. Am. Chem. Soc.* **1995**, *117*, 12498. Jung, B.; Karlin, K. D.; Zuberbühler, A. D. *J. Am. Chem. Soc.* **1996**, *118*, 3763. (e) Baldwin, M. J.; Ross, P. K.; Pate, J. E.; Tyeklár, Z.; Karlin, K. D.; Solomon, E. I. *J. Am. Chem. Soc.* **1991**, *113*, 8671.
 (5) (a) Magnus, K. A.; Hazes, B.; Tonthat, H.; Bonaventura, C.; Bonaventura, L.; Dauter, Z.; Kalk, K. H.; Hol, W. G. J. *Proteins: Struct., Funct. Genet.* **1994**, *19*, 302. (b) Tonthat, H.; Magnus, K. A. *J. Inorg. Biochem.* **1993**, *51*, 65. (c) Ling, J.; Nestor, L. P.; Czernuszewicz, R. S.; Spiro, T. G.; Fraczkiewicz, R.; Sharma, K. D.; Loehr, T. M.; Sanders-Loehr, J. *J. Am. Chem. Soc.* **1994**, *116*, 7682.

(6) Comba, P.; Hambley, T. W. *Molecular Modeling of Inorganic Compounds*; VCH: Weinheim, Germany, 1995.

Scheme 1



of potential energy functions and their parameterization, based on as large as possible sets of thermodynamic, vibrational spectroscopic, and/or structural experimental data; i.e., force field calculations basically are interpolations.^{6,7} Thus, the reliability of molecular mechanics modeling is strongly dependent on the quality of the basis set used for setting up the model. This may amount to a real problem in the study of specific and interesting questions, where experimental data are scarce, such as in the case discussed here. We try to show how a reasonable parameterization may be obtained with very little directly related structural data, we critically analyze this force field and the data obtained, and we deliberately communicate these results before being able to rigorously validate them, and before getting the chance of “fine tuning” the model, based on experimental studies that were initiated by these computations.

Results and Discussion

All structure optimizations were performed with MOME_C,⁸ using a published force field.⁹ The angular geometry around copper(II) was modeled based on 1,3-repulsive forces alone (Urey–Bradley approach^{8,9}). We stress that all force field parameters involving the metal center are dependent on the coordination geometry,⁷ and the parameters for distorted octahedral, square pyramidal, and trigonal bipyramidal geometries around copper(II) must be different. In the present study, we did not adjust for these effects, mainly because we know from previous work^{6,7,10} that the differences to be expected here must be rather small, and the resulting decrease in accuracy may not be relevant, based on the quality of the present parameterization. Also, for the present computations, we did not differentiate between intraligand bonds that are influenced by the metal center and bonds in the organic backbone of the ligand.⁶ Again, these effects are believed to be too small to be relevant for the present discussion.¹⁰ There are two other

Chart 2

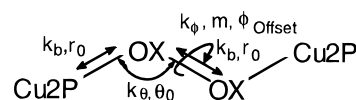


Table 1. Force Field Parameters for End-On (μ -Peroxo)dicopper(II) and -dicobalt(III) Compounds with Mixed Pyridine/Amine Donor Sets^a

Bond Distance Parameters		
bond type	force constant ^b (mdyn Å ⁻¹)	strain-free bond distance (Å)
OX–OX	3.25	1.430 for Cu2P 1.470 for Co3
Cu2P–OX	0.60	1.830
Co3P–OX	1.75	1.840
Valence Angle Parameters		
valence angle type	force constant ^b (mdyn Å rad ⁻²)	strain-free valence angle (rad)
Cu2P–OX–OX	0.50	1.911
Co3P–OX–OX	0.50	1.911
Torsion Angle Parameters		
bond torsion	force constant ^b (mdyn Å)	offset angle (rad)
OX–OX ^c	0.90	0.000

^a All other parameters are described in the text or given in the literature.⁹ ^b dyn = 10⁻⁵ N. ^c Periodicity 1.

important points in relation to the force field used here: (i) force field parameters in general are not transferable and highly correlated; i.e., additions to a set of parameters bear on the quality of the already available parameters; (ii) there is a difference between force fields based on structural experimental data (as were used for obtaining most of our parameters in the past^{8–10}), on thermodynamic data, or on vibrational spectroscopic data.^{6,7} The latter depend strongly on the steepness of the potential energy function (thermodynamics) and on the curvature (spectroscopy). It is important then to stress that our Co(III), Co(II), and Ni(II) hexamine force fields have been validated for thermodynamic studies (conformational analyses, redox potentials, stereoselectivities^{6,7,11,12}). Due to the cross-correlation of the parameters and to the fact that we use a constant parameterization for the organic ligands, there is some reason to hope that good-quality structural predictions will lead to reasonable predictions of thermodynamic properties.

The parameters for the study of (μ -peroxo)dicopper(II) compounds with pyridine and amine donor groups, not available so far in our force fields, are shown in Chart 2, which also gives the labeling of the atom types used in Table 1. As usual, the force constant for the torsional rotation involving the metal ion (L–Cu2P–OX–OX) was set to zero.^{6,9} For metal–ligand bonds involving some π character, this might be a questionable approach.¹⁰ However, so far this has not lead to appreciable artifacts in other studies,¹⁰ and the experimentally determined valence angles around the peroxide donor and the oxygen–oxygen distance in the published X-ray structure^{3a} indicate that the delocalization of electron density in the Cu–O bond is rather small (O–O: 1.43 (dicopper(II)), 1.47 Å (dicobalt(III); average over seven structures used for the parameterization); M–O–O: 107.6 (dicopper(II)); 112.3° (dicobalt(III); average over seven structures)). In the Urey–Bradley force field,⁹ the valence angles around the metal center are modeled by 1,3-interactions,

(7) Comba, P. in *Fundamental Principles of Molecular Modeling*, eds. Amann, A., Boeyens, J. C. A., Gans, W., Eds.; Plenum Press: New York, 1996; p 167.

(8) Comba, P.; Hambley, T. W.; Okon, N. MOME_C a Molecular Mechanics Package for Inorganic Compounds, Lauer & Okon, Heidelberg, Germany, 1995 (e-mail: CVS-HD@T-ONLINE.DE).

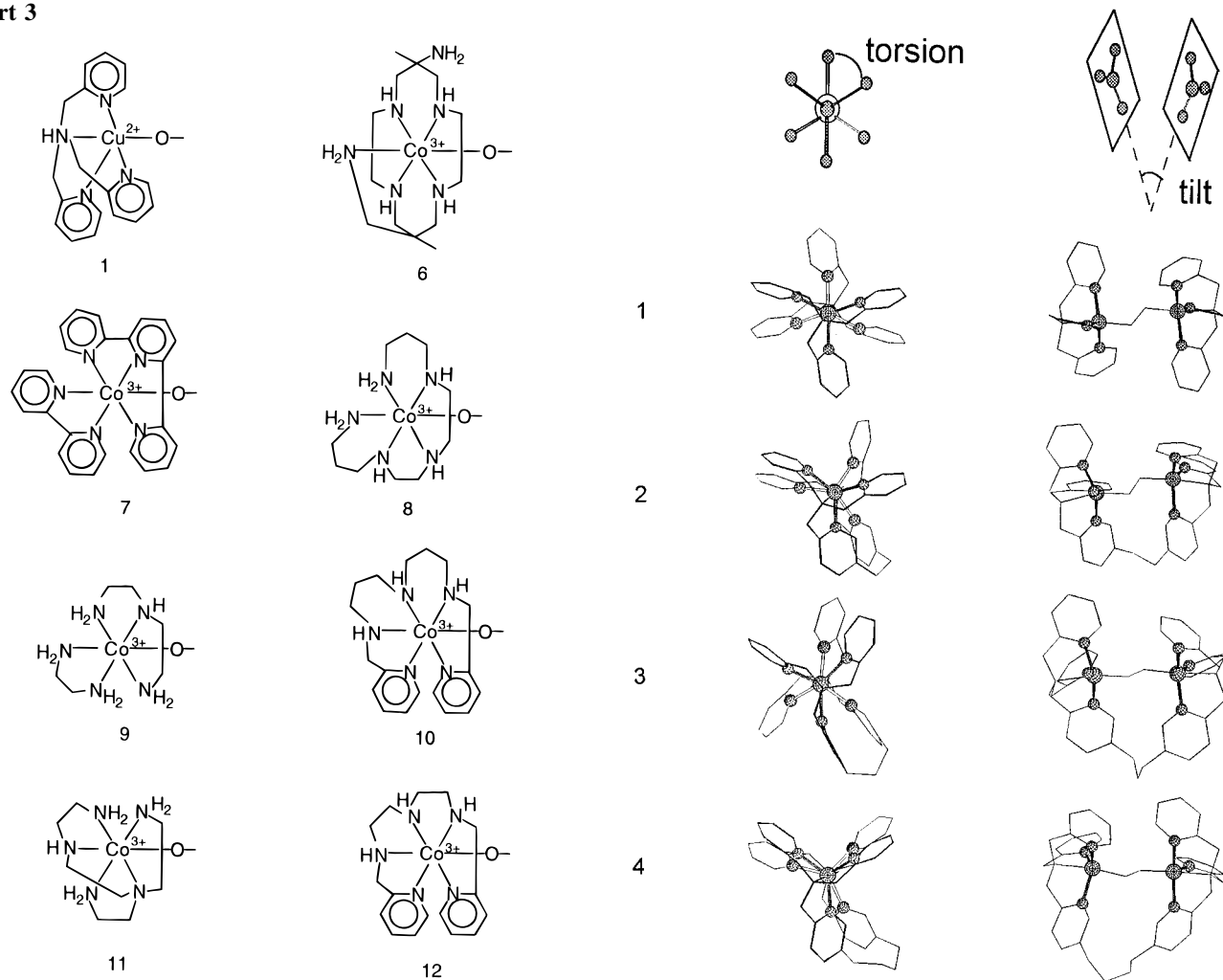
(9) Bernhardt, P. V.; Comba, P. *Inorg. Chem.* **1992**, *31*, 2638.

(10) Bol, J.; Buning, C.; Comba, P.; Stroehle, M., publication in preparation.

(11) Comba, P. *Coord. Chem. Rev.* **1993**, *122*, 1.

(12) Comba, P.; Sickmüller, A., submitted for publication.

Chart 3



and this does not require any specific parameterization in the present structures. Thus, the four critical sets of missing parameters include the copper(II)–peroxide stretching (Cu2P–OX), the peroxide stretching (OX–OX), the valence angle bending around the peroxide oxygen donor (Cu2P–OX–OX), and the torsion involving the peroxide unit (Cu2P–OX–OX–Cu2P). For the development of these four sets of parameters only one relevant, experimentally determined structure was available^{3a} (see **1** in Figure 1 and Table 2, below; the computed structure is shown in Figure 1). There is a much larger experimental data basis available for end-on (μ -peroxo)dicobalt(III) compounds. Although the corresponding oxygen–oxygen distances and the angular geometries around the peroxide donors are slightly different (see above and Table 2 below), parameter sets for end-on (μ -peroxo)dicobalt(III) amines were also developed, in order to put the force field on a slightly more sound basis, especially with respect to the torsion around the peroxide bridge, which turned out to be rather critical for the present study.

The new force field parameters are given in Table 1. The force constant for the peroxide oxygen–oxygen stretching potential (OX–OX) was determined from experimental vibrational spectroscopic data^{4c} (eq 1), and the corresponding ideal

$$\bar{\nu} = \frac{\sqrt{k/\mu}}{2\pi c} \quad (1)$$

bond distance was fitted to the experimental structure.^{3a} The same force constant was used for the corresponding cobalt(III) compounds, where the strain-free bond distance was fitted to

Figure 1. Strain energy-minimized structures end-on (μ -peroxo)dicopper(II) complex **1**, and of the four derivatives linked by different spacer groups ("torsion" (left column), view along a Cu...Cu axis; "tilt" (right column), side view; see also Table 3).

all end-on (μ -peroxo)dicobalt(III) structures with mixed pyridine/amine donor sets available in the Cambridge Structural Database (Chart 3). The computed O–O distances (see Table 2) indicate that the force constant used might be too stiff. Indeed, it is expected that the spectroscopic energy curve is steeper, and therefore the force constant is larger, than that used in the molecular mechanics calculations. However, in practice spectroscopic bond length deformation force constants are usually not significantly different from those used in MM.⁶ Therefore, on the basis of the rather small set of available data, we have decided to use here the spectroscopic parameter. The force constants used in our force field⁹ for valence angles around the donor atom are generally regarded to be independent of the metal center. Thus, we have used here the same parameters for the dicopper(II) and the dicobalt(III) complexes, fitted to the (μ -peroxo)dicopper(II) and the 7 (μ -peroxo)dicobalt(III) structures. Obviously, this approach neglects electron redistribution due to coordination to different metal cations,¹⁰ but

Table 2. Strain Energy-Minimized (and Observed) Bond Distances and Valence and Torsion Angles of the Computed M–O–O–M Fragments

structure	strain energy (kJ/mol)	M–O (Å)	O–O (Å)	M–O–O (deg)	M–O–O–M (deg)
1	86.27	1.86 (1.85)	1.43 (1.43)	110.3 (107.6)	180 (180)
6	156.08	1.88 (1.89)	1.47 (1.48)	113.7 (113.9)	172 (160)
7	146.67	1.88 (1.87)	1.47 (1.42)	113.0 (112.6)	178 (180)
8	150.07	1.90 (1.92)	1.47 (1.49)	115.9 (111.9)	180 (180)
9	89.20	1.88 (1.89)	1.47 (1.49)	113.1 (110.0)	179 (180)
10	188.99	1.89 (1.89)	1.47 (1.45)	113.6 (115.4)	173 (162)
11	129.02	1.88 (1.88)	1.47 (1.48)	112.6 (109.8)	179 (180)
12	129.72	1.88 (1.87)	1.47 (1.49)	113.9 (112.5)	175 (174)

Table 3. Computed Steric Strain and Structural Features of the (μ -Peroxo)dicopper(II) Compounds

compd (spacer)	A strain energy (kJ/mol)	B spacer-induced strain energy ^a (kJ/mol)	C rms-overlay of the chromophores ^b	D Cu···Cu (Å)	E Cu–O–O–Cu (deg)	F tilt ^c (deg)	G torsion ^d (deg)
1 (–)	86.27	0	0	4.42	180	0	60
2 (–CH ₂ CH ₂ –)	100.40	9.94	0.402	4.42	175	24	35
3 (–CH ₂ CH ₂ CH ₂ –)	95.36	3.66	0.345	4.43	176	12	49
4 (–CH ₂ CH ₂ CH ₂ CH ₂ –)	103.03	2.25	0.578	4.40	165	22	18
5 (–CH ₂ OCH ₂ –)	101.63	4.18	0.400	4.43	175	6	30

^a Difference of the strain energies of the optimized structures, after replacing the spacer groups by H-atoms, and of the strain energy of the computed structure of **1**. ^b Rms overlay of the N₃CuO₂CuN₃ fragment with the N₃CuO₂CuN₃ fragment of the calculated structure of **1**. ^c Angle between the calculated best planes through Cu(N_{py})₃. ^d Averaged torsion angle involving the N_{py}–Cu···Cu–N_{py} fragment.

artifacts due to this first-order approach are believed to be small.^{6,9,11} The stretching force constants for the Cu–O and Co–O bonds were set to values similar to those used for other metal–O,N,S potentials in the published force field⁹ (the published values for Cu(II)–O,N,S bonds are 0.7 ± 0.1 mdyn Å⁻¹, those for Co(III)–O,N,S are 1.60 ± 0.15 mdyn Å⁻¹). The corresponding strain-free distances were fitted to the experimentally observed structures. The potential of the torsion around the peroxo bridge was, together with the valence angles around the peroxide donors, believed to be of central importance. The corresponding parameters were fitted to available X-ray structures of the one dicopper(II) and the seven dicobalt(III) complexes. For the C–O–C fragment of the ether-linked ligand (**5**), the parameters of the published force field were used, except for the C–O strain-free bond distance, which was set to a value 0.1 Å shorter than the corresponding C–C parameter, similar to the corresponding differences in the MM2 force field¹³ ($k_{\text{b}}(\text{C–O}) = 5.000$ mdyn Å⁻¹ for the bond-stretching force constant and $r_0(\text{C–O}) = 1.400$ Å for the strain-free bond distance, $k_{\theta}(\text{C–O–C}) = 0.75$ mdyn Å rad⁻²). Tables 2 and 3 report the structural and thermodynamic results obtained, and the calculated structures of the end-on (μ -peroxo)dicopper(II) compounds are given in Figure 1. There is good overall agreement between all computed structures with the corresponding experimental data.

Strain energies are not absolute but relative parameters and only comparable within a set of isomers. Thus, the total strain energies of the refined molecules (column A in Table 3) are not of any direct use for the evaluation of the optimal size of the spacer group. In order to assess the strain of the (μ -peroxo)dicopper(II) products, induced by the four different spacer groups, these were replaced by H-atoms (attached with ideal geometries), after refining each of the four structures. Together with the parent structure **1**, this gave five slightly different structures of the same molecule, with the structural differences attributed to the spacer groups. The calculated strain energies of these structures are directly comparable and a measure for the spacer-induced strain energy (column B in Table 3). These parameters indicate that the strain induced by an ethyl spacer is significant and that the strain enforced by the bridge

diminishes with increasing length of the spacer. Considering the accuracy of computed strain energies in general, and that of the present case in particular, it is reasonable to argue that the spacer-induced strain is similar for the propyl-, butyl-, and ether-linked ligands (~3 kJ/mol) and significantly lower than that of the ethyl-linked ligand (~10 kJ/mol). Note, that the overall gain in free energy of the linked ligands **2–5** is also based on a favorable entropy effect. This diminishes with increasing size of the bridge, and this is neglected in our computations.

Four structural parameters are also listed in Table 3: the Cu···Cu distance, column D; the torsion around the peroxide bond, column E; the tilt angle of the two Cu(N_{py})₃ best planes, column F; the averaged torsional angle around the Cu···Cu axis, column G. The Cu···Cu distances of all dicopper(II) structures with linked ligands are very similar and close to identical with that of the parent molecule **1** (column D). The torsional angle around the peroxide bond of all structures are close to that of **1**, except for that with the butyl bridge (**4**), which is distorted by 15° (column E). The relative orientation of the two copper sites is described by the “tilt” and the “torsion”, given in columns F and G of Table 3 (see also Figure 1), and these seem to be rather sensitive to the geometry of the bridged ligands. The smallest distortions of the “tilt” are found for the two ligands with three-atom bridges but only for the propyl-bridged ligand **3** is the “torsion” close to that of the parent molecule **1**. This also emerges from the rms shifts between the computed chromophores of the bridged species and that of the parent compound (column C in Table 3). In summary, the computed structures (Figure 1, Table 3) show that the strain induced by the spacer groups involves a balance between “torsion” and “tilt” of the two chromophores, the Cu···Cu separation, and the torsion around the peroxo bridge. The structural features and thermodynamic considerations (spacer-induced strain energies) indicate that the propyl-linked ligand is the most favorable for stabilizing the (μ -peroxo)dicopper(II) product.

Conclusions

The experimental data^{4c} indicated a decrease in enthalpy of up to 50 kJ/mol for the ethyl-linked species **2**. Our force field is mainly based on structural data, and it therefore does not allow for an accurate thermodynamic analysis. However, it is hard to believe that the steepness of the potential energy curves

(13) Weiner, S. J.; Kollman, P. A.; Nguyen, D. T.; Case, D. A. *J. Comput. Chem.* **1986**, *7*, 230.

defined by our current force field is underestimated by 1 order of magnitude (vide supra). An important aspect is that the experimentally determined energy difference of 50 kJ/mol relates to the difference between the two unlinked mononuclear and the ethyl-linked dinuclear compounds, reacting to the (μ -peroxo)dicopper(II) species; i.e., the loss in enthalpy may also reflect some strain energy differences in the copper(I) compounds. This possibility has not been evaluated in our analysis. We suggest that a decrease in the O_2^{2-} to Cu(II) bonding energy may also contribute to the apparent discrepancy. The orbitals of the free peroxide ion, responsible for the bonding interaction, are a double-degenerated set of antibonding π^* orbitals, split into π_σ^* (σ bonding with the half-filled Cu(d_z^2) acceptor orbital) and π_ν^* , upon binding to Cu(II). Charge transfer transitions associated with these orbitals have been studied in detail^{4e} for the unlinked dimer. It is of interest that a significant shift to lower energy is observed for both components of the $\pi^* \rightarrow$ Cu(d_z^2) transitions for the ethyl linked dimer (λ_{\max} (LMCT): (1) 525, 590 nm; (2) 540, 600 nm),^{4c-e} indicating a decrease of orbital overlap, possibly due to the distorted geometry. It then

emerges that both the increase in strain induced by the ethyl link *and* the distortion of the Cu–peroxo–Cu geometry are contributing to the decreasing stability of the end-on peroxo dimer. The results presented in Table 3 indicate that for the four ligands with different links both effects, i.e., steric strain and decreasing orbital overlap, are minimized with a propyl spacer group.¹⁴

Acknowledgment. We gratefully acknowledge financial support by the Deutsche Forschungsgemeinschaft and the Fonds der Chemischen Industrie.

Supporting Information Available: Tables of Cartesian coordinates of the five computed dicopper(II) and the seven computed dicobalt(III) structures (21 pages). Ordering information is given on any current masthead page.

IC961317W

-
- (14) *Note added in proof:* A recent experimental study with **5**¹⁵ supports our conclusions based on molecular modeling.
(15) Karlin, K. D.; Lee, D.-H.; Kaderli, S.; Zuberbühler, A. D. *J. Chem. Soc., Chem. Commun.* **1997**, 475.